CHAPTER 8

Energy Efficiency Metrics in Membrane Distillation

David M. Warsinger[*], Sina Nejati, and Hamid Fattahi Juybari

*Birck Nanotechnology Center, School of Mechanical Engineering,
Purdue University, West Lafayette, IN, USA*

8.1. Introduction

New technologies continue to grow and emerge to address emerging challenges to water and energy resources caused by population growth and climate change.[1,2] In water-stressed regions, desalination technologies to extract freshwater from seawater or brackish water are well-established, but efforts continue to make them more efficient and applicable to more water source types.

Membrane distillation (MD) is an emerging thermal desalination technology in which feed water evaporates at a membrane that permits water vapor to pass while preventing any liquid water to penetrate. The vapor is then condensed on the other side of the system producing pure water (Fig. 8.1).[3] MD offers unique advantages over other technologies including the ability to scale down the system to smaller sizes, being fouling resistant, the ability to work at low temperatures, and potentially having competitive efficiencies compared to other thermal desalination technologies like multi-effect distillation (MED) and multi-stage flash (MSF). Deshmukh *et al.*[4]

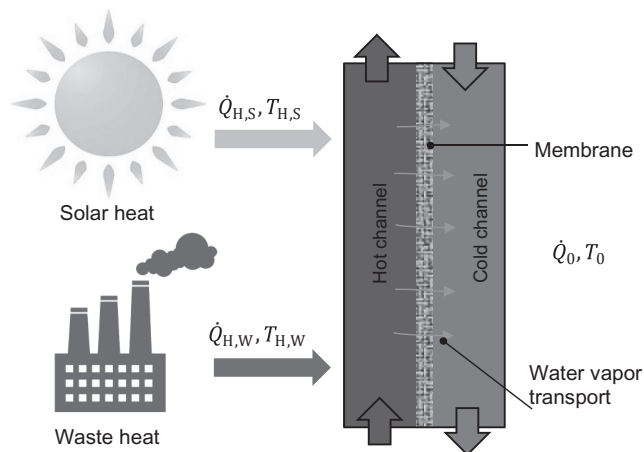[*]Corresponding author: david.warsinger@gmail.com

Fig. 8.1. Principle of MD process utilizing solar and waste heat as two energy sources.

showed that in large scales ($>1000\,\mathrm{m}^3$ day^{-1} water production), MD is less efficient compared to MED and MSF. However, this trend is reversed for small scale systems. MD systems can operate effectively at lower temperatures than most other industrial processes ($<80°$C).[5,6] So, MD could use solar and waste heat (Fig. 8.1),[7] and it would be a low carbon desalination technology.[8]

These advantages for low temperatures and small sizes have led MD applications to substantially consider the two underused power sources of waste heat and renewable solar energy. Researchers have also proposed other energy sources with higher amounts of available work, such as Joule heating. However, the energy source chosen can drastically impact the overall thermodynamic efficiency, which is often ignored.[4]

MD systems need further efficiency improvements to truly takeover the niches for thermal technologies, but the best implemented systems[9] remain well below the performance of the best theoretical systems. These systems are complex, as their performance depends on both system-level inputs such as the temperatures and total energy flows,[10] as well as micro-scale transport processes impacted by local properties such as membrane conductivity. In order to advance MD systems to their potential, a better understanding and implementation of MD efficiency is needed.

This chapter aims to unify the various metrics for MD efficiency. Here, we organize, categorize, and include the equations to convert between types of efficiencies, and explain the best uses of each type to maximize performance. To do so, this work chapter divides MD metrics into two primary categories: local and system level metrics. Additionally, it provides modeling results of representative figures that conveys how the metrics are inter-related.

8.2. MD Energy Efficiency Metrics

In this section we present the main performance metrics for MD clearly and concisely, while conveying when to use each one. The sections are organized by thermodynamic category.

In this section, the main metrics are categorized into local and system level groups:

Local:

- Flux
- Thermal efficiency

System level:

- First law efficiency: gained output ratio (GOR), evaporation efficiency, specific energy consumption (SEC)
- Heat transfer effectiveness
- Number of transfer units (NTU)
- Second law efficiency

8.2.1. *Flux*

The permeate flux J of membrane distillation is one of the most significant metrics for the comparison of any membrane technology.[10] Simply, it is the flow rate of permeate through the membrane, defined as:

$$J \equiv \frac{\dot{m}_{\mathrm{p}}}{A} \tag{1}$$

For MD, flux is driven by the vapor pressure difference, often simply described as:
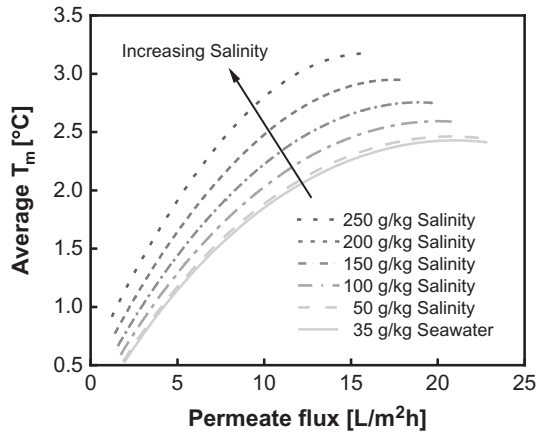
$$J = B_{\mathrm{m}}\Delta P_{\mathrm{vap}} \tag{2}$$

Fig. 8.2. Average temperature difference across the membrane with permeate flux, showing impact of driving temperature across the membrane ΔT_m and salinity. Conditions varying module length $L = 0.1$ m to 12 m at salinities ranging from seawater, 35 g/kg, to 250 g/kg in an AGMD system. Membrane permeability coefficient is set to $B = 2 \times 10^{-10}$ kg/m Pa s, $T_{c,i} = 25°$C, $T_{f,i} = 85°$C, $\delta_m = 0.2$ mm and $d_{gap} = 1$ mm represent the parameters used for the computations.

where $\dot{m}_p$ is the mass flow rate of permeate, A is the membrane area, B_m is membrane permeability, and ΔP_{vap} is the vapor pressure difference across the membrane. This term ΔP_{vap} is affected by temperature and salinity, but not with absolute pressure.

Figure 8.2 shows the impact of key parameters on membrane flux. The driving force for permeate flux, ΔP_{vap}, is a direct thermodynamic function of the temperature difference across the membrane, ΔT_m. However, increasing salinity reduces the vapor pressure on the feed side.

As membrane area is a key capital cost in MD, flux is an essential and easy-to-measure and almost universally used parameter for membrane distillation.

8.2.2. *First-law efficiency: GOR, evaporation efficiency, SEC*

The performance of thermal desalination systems is often described as a function of energy input, regardless of energy type: such a metric is a "First-law efficiency," as it considers only energy, similar to the

first law of thermodynamics. Of these, the principle metric typically used to describe these is the GOR. This dimensionless parameter is a ratio of enthalpy of evaporation for the separated water to actual input heat for separation, or:

$$\text{GOR} \equiv \frac{\dot{m}_{\text{p}} h_{\text{fg}}}{\dot{Q}_H} \tag{3}$$

where h_{fg} is the water enthalpy of vaporization (2257 kJ/kg), and $\dot{Q}_{\text{H}}$ is the total heat energy input.

GOR shows how many times the enthalpy of evaporation is reused within the system. Essentially, it directly reflects the energy efficiency and cost of energy used within the system. As a result, the higher the GOR in MD system, the better, although practical design costs often lead to trade-offs with flux which will be discussed later.

Evaporative systems without heat recovery, such as some lab-scale MD systems, or technologies like most steam evaporators and solar stills, often have a GOR between 0 and 1. For example,
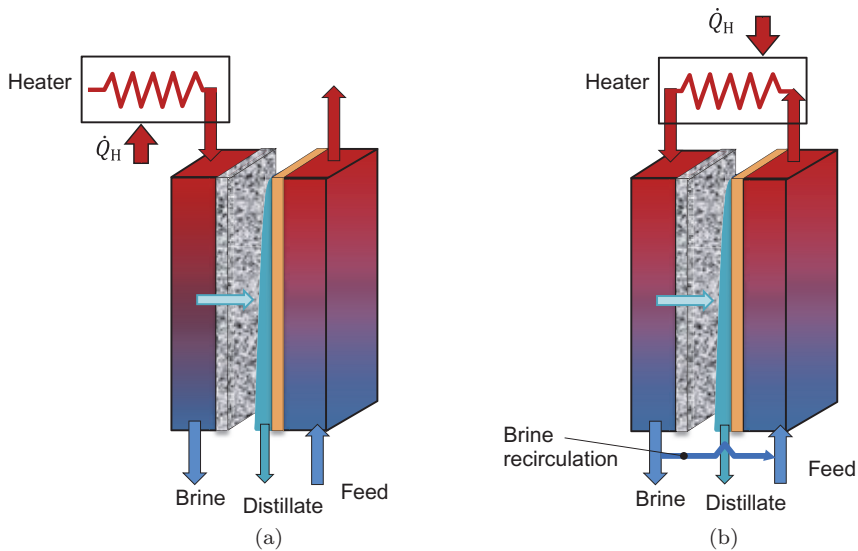

Fig. 8.3. The schematic of (a) separated hot and cold feed at MD (traditional MD setup, GOR < 1) and (b) preheating feed inlet in MD and brine recirculation, necessary for reasonable efficiency (GOR > 1).

Fig. 8.3(a) shows an MD system without heat recovery of the cooling stream, limiting the GOR below 1. Therefore, practical MD systems achieve GOR values greater than 1, by recovering the latent heat of the cooling and brine streams via preheating; Fig. 8.3(b). In the preheating loop, most of the brine heat could be reused by increasing the module length (membrane area), or by multi-stage design. The configuration shown has internal heat recovery (within the membrane module), which is seen in the MD configurations known as air gap (AGMD), permeate gap (PGMD), and conductive gap (CGMD). Recovery of latent heat can also be done with an external heat exchanger,[11] which is seen in the MD systems known as direct contact (DCMD) and vacuum (VMD).[12–17]

Notably, there tends to be a maximum GOR for a given MD operating conditions, based on the membrane area made available (which in turns alters flux). This can be seen as GOR vs flux peaks (Fig. 8.4). The primary limitation causing these peaks is the boiling point elevation (BPE), a term which describes vapor pressure reductions from higher salinity in the feed side. For a given salinity,
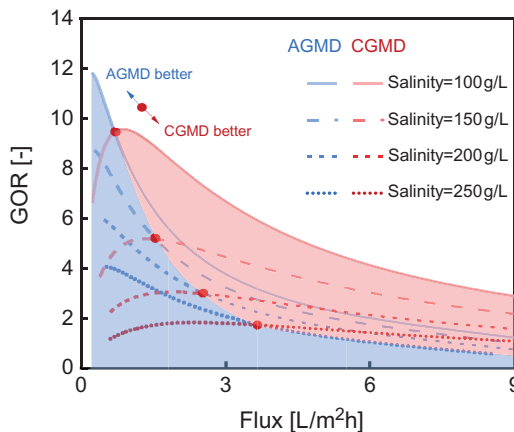

Fig. 8.4. GOR vs flux for CGMD and AGMD over a range of salinity.[13,18] Red dots indicate the trade-off conditions at which AGMD or CGMD begins to dominate with the superior GOR vs flux frontier. Membrane permeability coefficient is set to $B = 2 \times 10^{-10}\,\mathrm{kg/m\,Pa\,s}$, $T_{\mathrm{c,i}} = 25°\mathrm{C}$, $T_{\mathrm{f,i}} = 85°\mathrm{C}$, $\delta_{\mathrm{m}} = 0.2\,\mathrm{mm}$ and $d_{\mathrm{gap}} = 1\,\mathrm{mm}$ represent the parameters used for the computations.

to have enough vapor pressure to drive flux, there needs to be a higher temperature on the feed side; this ΔT is the BPE. As a result, the maximum possible GOR for a given system is a strong function of salinity. Overall, this comparison is a great way to go about optimizing performance.

However, the first-law metrics like GOR have a serious drawback; they do not consider the available work (exergy) that a heat stream may have. For a thermal process, this available work increases as temperature difference increases. GOR, therefore, is not fully reliable when comparing systems of substantially different operating temperatures or energy input types. As such, GOR is referred to as a *First Law Efficiency* metric, as it considers only the first law of thermodynamics and neglects the *Second Law of Thermodynamics*, which includes entropy. Because of this significant limitation, these first law metrics are largely useful in comparing systems with the same energy sources.

Notably, there are several other first law metrics that can be directly converted to GOR.

However, some reporting of solar evaporation efficiency ignores components of $\dot{Q}_{\text{vap}}$ or $\dot{Q}_{\text{total}}$, they may not match.

For related systems, especially those using solar power, an *evaporation efficiency* is often given: these numbers are usually identical to the thermal efficiency, where $\dot{Q}_{\text{H}}$ is a solar energy input. The three metrics converge in systems with negligible heat recovery, such as in small coupon modules or those without a flowing preheating stream. In those cases, $\dot{Q}_{\text{vap}} = \dot{Q}_{\text{total}}$, and the GOR and thermal efficiency converge. However, for real MD systems with heat recovery, the metrics may not correlate with one another. Usually a full model of an MD module is needed. Such an approach can allow for GOR calcualted from small systems. Those figures are typically below 100% (a GOR of 1) since they usually lack the heat recovery.

Another closely related performance metric is the SEC, or specific energy consumption, which is the energy input used to produce $1\,\text{m}^3$ of distillate (i.e. ratio of energy supplied to the volume of produced fresh water). The SEC varies from about 20 to $9000\,\text{kWh/m}^{4,19}$

depending on the type and size of the MD system, feed processed water, energy source, energy recovery systems, etc.

The specific energy consumption (SEC)[20] can be calculated with:

$$SEC = \frac{\dot{Q}_H}{\dot{m}_p} = \frac{h_{fg}}{GOR} \tag{4}$$

While these first law metrics are simply related by a constant, they are the reciprocal of one another, so for SEC, lower values are better, unlike the case of GOR.

Usually, the SEC is much higher for small laboratory MD systems compared to larger pilot plants with greater membrane areas.

8.2.3. *Thermal efficiency*

While system-level metrics like GOR are helpful in system design, they are not as easily applied to design choices that are local rather than system-level, such as material and channel depth choices. For such local considerations, the MD thermal efficiency η_{th} is the standard metric and helps with understanding tradeoffs with heat and mass transfer. Researchers find this metric particularly useful as it can bridge lab-scale results to meaningful implications for large systems. The MD thermal efficiency describes how much of the heat transfer between the feed and preheating channel is used to enact desalination, as a fraction of total heat transfer, which includes conduction losses. More specifically, thermal efficiency is defined as the fraction of energy transferred across the membrane as pure vapor transport[21]:

$$\eta_{\text{th}} \equiv \frac{\dot{Q}_{\text{vap}}}{\dot{Q}_{\text{total}}} \tag{5}$$

where $\dot{Q}_{\text{total}}$ is composed of $\dot{Q}_{\text{vap}}$ and $\dot{Q}_{\text{cond}}$. Heat transfer by conduction across the membrane ($\dot{Q}_{\text{cond}}$) is a loss mechanism; Ideally η_{th} approaches 1, meaning that all the energy supplied to the process should be used for the evaporation ($\dot{Q}_{\text{vap}}$) that causes desalination.[21]

The thermal efficiency can be calculated easily from lab-scale experimental data, as $\dot{Q}_{\text{vap}}$ is simply a function of the permeate flow rate and enthalpy of evaporation, while the denominator can

be described as a function of total enthalpy removed by the feed stream, which can be described by the heat capacity c_p:

$$\eta_{\text{th}} \approx \frac{\dot{m}_{\text{p}} h_{\text{fg}}}{c_p(\dot{m}_{\text{f,i}} T_{\text{f,i}} - \dot{m}_{\text{f,o}} T_{\text{f,o}})} \tag{6}$$

where the temperatures are taken at the inlet and outlet of some portion of the feed side, as shown in Fig. 8.5.

The thermal efficiency is effectively a measurement of desired thermal transport local to some membrane multilayer sandwich that includes the membrane and major channels. It is thus an excellent parameter for optimizing material choices and layer thicknesses. To improve it, one must increase the resistance to conduction, and/or decrease the resistance to mass transport. Therefore, typically the thermal efficiency can be increased by reducing the thermal conductivity of the membrane, increasing membrane thickness, or by using an air gap. Alternatively, design changes to aid mass transport through the membrane (or air gap) such as a more porous or permeable membranes, can also increase it.
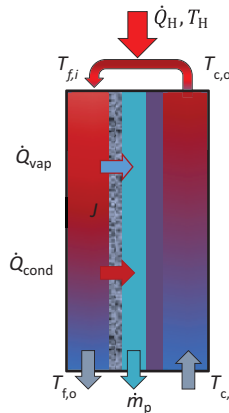

Fig. 8.5. Heat input and heat recovery in the module, showing key parameters for calculated the thermal efficiency of membrane distillation, η_{th}. The heat flow rates shown are those that define η_{th}, and the feed temperatures shown can be used to easily calculate the overall thermal efficiency η_{th}, or the heat transfer effectiveness ε for the system.

However, as it does not consider system-level performance, η_{th} must be used in conjunction with other system-level efficiency metrics, to give any information on optimizing performance. As explained in the following sections, it can be used as a model input to help calculate the other metrics, a use that more researchers need to understand and implement.

8.2.4. *Heat recovery parameter (ε-NTU)*

While other performance parameters indicate total energy use (GOR) or local heat transport (η_{th}), performance parameters that describe operating conditions and system sizing are needed. Two such parameters can be applied from the primary analysis approach for heat exchangers,[10] as MD itself is a heat exchanger with a membrane in the middle. These parameters are the heat transfer effectiveness ε, and the Number of Transfer Units, or NTU; the approach using these parameters is referred to as ε-NTU.

The heat transfer effectiveness ε[22] measures how effectively heat is transferred across the MD module from feed to the cold side, as a fraction of 1, where 1 would be a maximum enthalpy increase for the cold stream. The parameter ε is therefore defined as an enthalpy ratio, but since specific heat is relatively constant in MD, ε can also be expressed in temperature differences only:

$$\varepsilon \equiv \frac{\dot{Q}}{\dot{Q}_{\max}} = \frac{h_{\text{c,o}} - h_{\text{c,i}}}{h_{\text{f,i}} - h_{\text{c,i}}} = \frac{T_{\text{c,o}} - T_{\text{c,i}}}{T_{\text{f,i}} - T_{\text{c,i}}} \tag{7}$$

where $\dot{Q}$ is heat transfer between inlet and outlet streams, h is enthalpy, and the subscripts c, f, i and o represent the cold, feed, inlet, and outlet respectively, as shown in Fig. 8.5. The heat transfer effectiveness ε approaches 1 as the temperature difference across the membrane approaches zero; performance approaches this limit with larger areas (and lower fluxes) and reduced heat transfer resistance in the channels, but boiling point elevation (a result of higher feed salinity) provides an upper limit on values of ε.

This effectiveness (ε) heat exchanger metric is typically used in conjunction with its partner metric, the Number of Transfer Units

(NTU). NTU is a dimensionless system size metric that includes heat transfer. NTU is related to J as they both describes system size, but this new metric is dimensionless which makes it easier to transfer insights across designs. The NTU of an MD module is defined as:

$$\text{NTU} \equiv \frac{UA}{\dot{m}c_p} = \frac{T_{\text{c,o}} - T_{\text{c,i}}}{T_{\text{f,i}} - T_{\text{c,o}}} \tag{8}$$

where, U is the overall heat transfer coefficient across the MD module between cold and hot streams measured in $\text{W/m}^2\,\text{K}$, and c_p is the specific heat. The concept of NTU originally appeared in the heat exchanger literature for heat exchanger sizing and rating. Larger values of NTU indicate larger system size and better heat transfer performance, whereas smaller J values usually indicate a larger system size only but can be caused by inferior heat transfer.

Like in heat exchanger analysis, the overall heat transfer coefficient times area, UA, is equal to the inverse of the thermal resistance. Therefore, it can be readily calculated using the resistances in MD, including boundary layer resistance in the cold and hot streams, the effective resistance of the membrane, and the heat conduction resistance of the gap. As a result, the overall heat transfer coefficient U can be expressed as:

$$\frac{1}{U} = \frac{1}{h_{\text{f}}} + \frac{1}{h_{\text{eff,m}}} + \frac{d_{\text{gap}}}{k_{\text{gap}}} + \frac{1}{h_{\text{c}}} \tag{9}$$

where h_{f} is the heat transfer coefficient in the feed, h_{c} is the heat transfer coefficient in the cold channel and $h_{\text{eff,m}}$ is the effective heat transfer coefficient of the membrane. With this term, the ε-NTU framework can be used to directly relate MD performance gains with thermal enhancements, including flow rates, material choices, and channel dimensions.

Figure 8.6 shows the GOR of MD at various salinity levels as a function of system NTU. Beyond a certain system size, the GOR decreases. There exists a value of (NTU^*) beyond which the GOR starts declining. At larger system sizes, the flux is also lower since the overall driving temperature difference is lower. This means operating
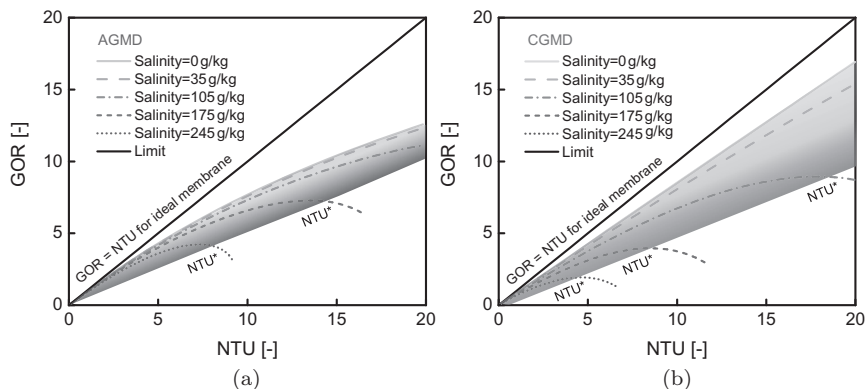
Fig. 8.6. GOR as a function of the heat exchanger dimensionless area parameter NTU (number of transfer units), for (a) AGMD and (b) CGMD at varied salinity. Shaded regions show realistic performance, with the darker bottom indicating the highest GOR (peak performance). These peak values represent dimensionless areas (NTU*) for best performance for each technology, with values to the left of the peak (lighter shading) saving on area cost, and values to the right of each peak are no-go design areas. Shorter module lengths (smaller NTU) have to be used when treating high salinity water with MD.[18] The parameters used for the computations were set to a membrane permeability coefficient is set to $B = 2 \times 10^{-10}$ kg/m Pa s, $T_{c,i} = 25^\circ$C, $T_{f,i} = 85^\circ$C, $\delta_m = 0.2$ mm and $d_{gap} = 1$ mm.

beyond (NTU*) leads to both a lower GOR and lower flux and hence should be avoided.

The dotted lines show that the simplified HX model is valid for high salinity as well. The existence of (NTU*) is indicated by the results from the simplified HX model as well. As a result, we attempt to use this model to determine the (NTU*) to choose safe operating conditions and system design.

For both MD and classic heat exchanger analysis, ε-NTU provides a fast and elegant system-level performance metric. Values of ε in MD modules approaching 1 indicates excellent heat recovery. However, in practice, high ε may mean a low ΔT across the membrane, and thus a small driving force (ΔP_{vap}) and smaller flux (J). Therefore, in optimizing design, comparing ε to a performance metric that considers system size (A, NTU, and J) is useful. In practice, computing NTU values can allow researchers to analyze how given material designs and channel geometries (which result in a given heat transfer effectiveness U) would perform in larger or smaller systems.

8.2.5. *Second law efficiency*

The second law of thermodynamics allows for the most fundamental and universal analysis of energy efficiency. In such analysis, it is often convenient to compare exergy rather than energy.

The concept of exergy, often called available work, is defined as the possible work we can extract from an energy source (in this case, heat) that interacts with the environment's end state. For desalination processes where this exergy difference is an energy barrier to overcome, it is often called the work of separation, $\dot{W}_{\text{least}}$. The actual work used by the process is denoted by $\dot{W}_{\text{sep}}$, and the two together define the second law efficiency for a separation process;

$$\eta_{\text{II}} \equiv \frac{\dot{W}_{\text{least}}}{\dot{W}_{\text{sep}}} = \frac{\text{Exergy}}{\dot{W}_{\text{sep}}} \tag{10}$$

Exergy analysis in recent years is a term called second-law efficiency. Second law efficiency, in contrast to the metrics such as first law efficiency (e.g. GOR), is a universal tool to describe the thermodynamic efficiency in any desalination processes, capable of comparing different desalination technologies with different energy sources and heat temperatures.

In the second law efficiency analysis, the heat source (Fig. 8.7) can be described as a function of the enthalpies h_{fg} of the permeate; this describes the first law of thermodynamics.
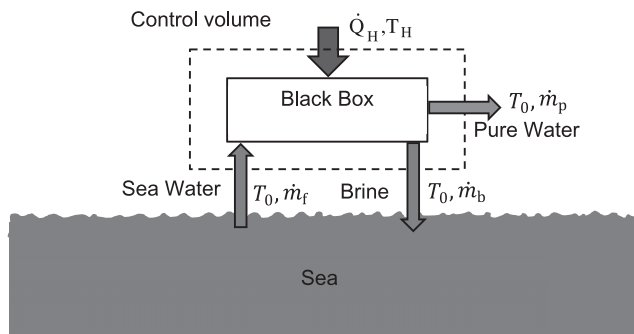

Fig. 8.7. A black box desalination system and control volume is useful for second law efficiency (η_{II}) analysis.[23] η_{II} is agnostic to the process itself and can be calculated with just the input and output streams. For desalination, the minimum least work between the streams is a function of the salinity and recovery ratio of pure water from seawater.

Here, the first law of thermodynamics is written as

$$\dot{Q}_{\mathrm{H}} - \dot{Q}_0 = (\dot{m}h)_{\mathrm{p}} + (\dot{m}h)_{\mathrm{b}} - (\dot{m}h)_{\mathrm{sw}} \qquad (11)$$

where $\dot{Q}_{\mathrm{H}}$ is the input energy at T_{H}, $\dot{Q}_0$ is the heat rejected to the environment at T_0, and the second law of thermodynamics is written as:

$$\frac{\dot{Q}_{\mathrm{H}}}{T_{\mathrm{H}}} - \frac{\dot{Q}_0}{T_0} = (\dot{m}S)_{\mathrm{p}} + (\dot{m}S)_{b} - (\dot{m}S)_{\mathrm{sw}} + \dot{S}_{\mathrm{gen}} \qquad (12)$$

The relative magnitude of entropy generation $\dot{S}_{\mathrm{gen}}$ is useful to understand the magnitude of efficiency losses. Using these laws, the work for a separation process like desalination can be described in a useful form that relates the work of separation, normalized by permeate production $\dot{m}_{\mathrm{p}}$, with the least heat for a process, and the flow described by the Gibbs free energy g of the liquid streams;

$$\frac{\dot{W}_{\mathrm{sep}}}{\dot{m}_{\mathrm{p}}} \equiv \left(1 - \frac{T_0}{T_{\mathrm{H}}}\right) \frac{\dot{Q}_{\mathrm{H,sep}}}{\dot{m}_{\mathrm{p}}} = (g_{\mathrm{p}} - g_{\mathrm{b}}) - \frac{1}{RR}(g_{\mathrm{sw}} - g_{\mathrm{b}}) + T_0 \frac{\dot{S}_{\mathrm{gen}}}{\dot{m}_{\mathrm{p}}} \qquad (13)$$

where $RR(=\dot{m}_{\mathrm{p}}/m_{\mathrm{f}})$ is the recovery ratio, and the last term describes exergy destroyed by the process.

To provide further clarity, one can visualize these thermodynamic flows through the membrane in an MD system (Fig. 8.8).

Figure 8.9 shows the relation of heat, entropy and exergy transfer in membrane distillation according to temperature difference between cold (T_{c}) and hot side (T_{f}). The first law of thermodynamics dictates that the heat flux $\dot{Q}$ is the same across both sides. However, entropy increases as heat transfers across a temperature gradient- this is the primary cause of exergy destruction, also known as the loss of available work, in membrane distillation. Every occurrence of heat transfer across temperature gradients causes such losses: as MD approaches theoretical ideals, these temperature gradients approach zero, and the $\dot{Q}$ from conduction across the membrane also approaches zero.
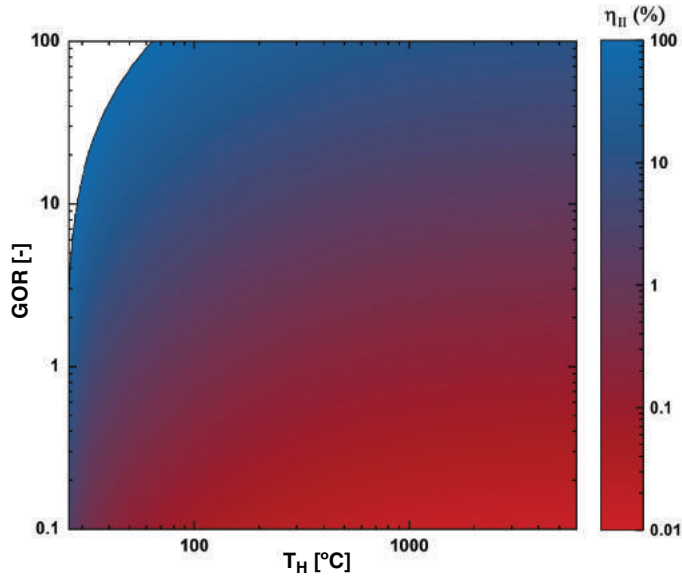
Fig. 8.8. Conversion plot for seawater desalination between second law efficiency η_{II} and first law efficiency (GOR) calculated for the case of an environmental temperature at $25°C$ and at $RR = 0$; and $\dot{W}_{least}/\dot{m}_{p} = 2.6\,kJ/kg$ and salinity $35\,g/kg$. Results are derived from $\eta_{II} = GOR \times \frac{\dot{W}_{least}}{\dot{m}_{p} h_{fg}} \times \frac{1}{1 - \frac{T_0}{T_H}}$

8.2.6. *Relating performance parameters to one another*

The following subsection goes over equations that can be used to relate the efficiency metrics to one another. More thorough discussion and derivations can be found in previous work by the authors and collaborators.[10]

The second law efficiency can be related to the first law metrics (GOR etc) by using Eq. 10 (which relates work to heat through the temperatures) and the definitions for both efficiencies.

The first law metrics (GOR etc.) can also be related to the thermal efficiency η_{th} and the framework ε-NTU. The standard MD configurations with internal heat recovery (AGMD, PGMD, CGMD, and similar systems) provide straightforward conversions for relating GOR in terms of η_{th} and ε as follows:

$$\text{GOR} = \eta_{th} \times \frac{\varepsilon}{1 - \varepsilon} \tag{14}$$
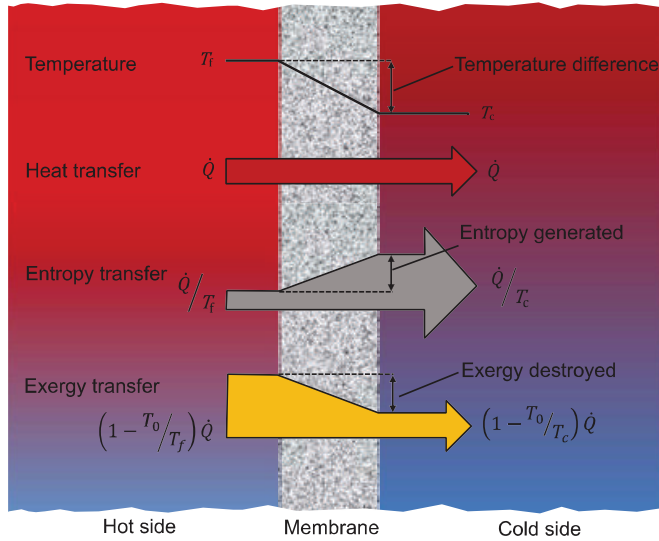
Fig. 8.9. Relation between energy, exergy, and entropy transfer across the membrane in MD.

ε can then be evaluated[24] assuming a perfect counter-flow heat exchanger as:

$$\varepsilon = \frac{NTU}{1 + NTU} \tag{15}$$

With this, the GOR expression derived earlier becomes:

$$GOR = \eta_{\text{th}} \times NTU \tag{16}$$

η_{th} can be evaluated as the fraction of the heat transferred through the mass transfer resistance as:

$$\eta_{\text{th}} = \frac{Bh_{\text{fg}}\Delta p_{\text{m}}}{Bh_{\text{fg}}\Delta p_{\text{m}} + \frac{k_{\text{m}}\Delta T_{\text{m}}}{\delta_{\text{m}}}}$$

$$= \frac{1}{1 + \frac{k_m}{\delta_{\text{m}} Bh_{\text{fg}}} \frac{\Delta T_{\text{m}}}{\Delta p_{\text{m}}}}$$

$$= \frac{1}{1 + \frac{k_{\text{m}}}{\delta_{\text{m}}} \frac{1}{h_{\text{m}}^{\text{mass}}}} \tag{17}$$

where $h_{\mathrm{m}}^{\mathrm{mass}}$ is heat transfer coefficient corresponding to vapor transfer across the membrane.

Inspired by the ε-NTU method, η_{th} and ε are rewritten in terms of the transport resistances within the MD system. A single stage membrane distillation module resembles a counter-flow heat exchanger with hot brine and pure product transferring energy into the cooler feed, thereby preheating it. Using similarities with heat exchangers, simplified effectiveness-MTU (mass transfer units) models for reverse osmosis[25] and pressure retarded osmosis systems[26] have also been developed. The overall heat transfer coefficient has been introduced and used to evaluate DCMD flux several times in the literature.[27] Other researchers[28] have used metrics similar to NTU, such as the particular membrane area multiplied by a transfer coefficient.

8.2.7. *Efficiency limits*

With many efficiency metrics, it is critical to convey a clear approach for best optimizing MD systems. Simply put, the capital costs (CapEx) per MD (membrane area) directly relate to flux J, so flux should be maximized. Meanwhile, the operating costs (OpEx) are often readily available in terms of energy input costs, which simply relate to first-law metrics such as GOR. Therefore, GOR vs flux curves can describe the primary tradeoff in MD systems, while other metrics can be used to optimize systems to maximize these curves. Notably, if comparisons are needed to other sources of energy, or energy inputs of different temperature, 2nd law analysis approaches become far more appropriate, with the downside of a slight increase in complexity.

The next line of questioning is just how high each metric can get, and under what conditions this would occur. The fractional metrics (ε, η_{th}) obviously can't approach one, but they can get quite close in well-designed systems. Second law efficiency η_{th} is capped at 100%, but thermal desalination systems very rarely get above 15%, due to significant exergy destruction, especially from heat transfer across temperature gradients. Interestingly, for an ideal membrane, GOR = NTU, but for achievable systems, there is usually a maximum NTU beyond which GOR will decrease. This means
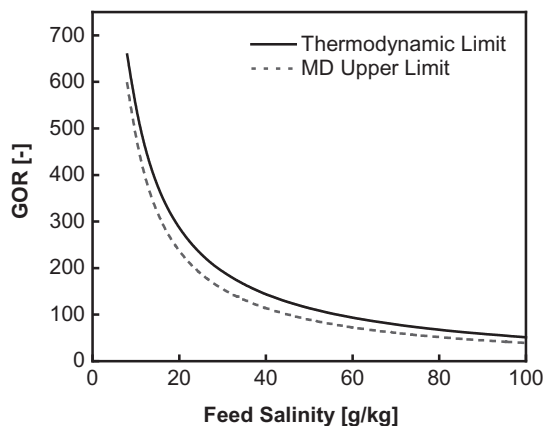
Fig. 8.10. Theoretical limits of MD system energy efficiency given perfect membranes ($\eta_{th} = 1$), perfectly insulating membrane, infinite thermal conductivity in the channels, and optimized design.[10,18]

that beyond a certain membrane area, more membrane area degrades performance, so NTU should never exceed this value, or conversely, the other area parameter, flux J, should never be below the value yielding maximum GOR.

As seen in Fig. 8.10, $GOR_{max,MD}$ is bounded by $GOR_{max,thermodynamic}$. One reason for lower $GOR_{max,MD}$ is that the boiling point elevation varies along the module length. As a result, vapor flux is driven by a non-zero driving force, generating entropy elsewhere. Both η_{th} and ε are lower for real MD systems since the membrane is not a perfect insulator and the area of the system is finite. As a result, real GOR values are at least an order of magnitude lower than the maximum possible GOR, leading to a second law efficiency of less than 10% as observed by Mistry *et al.*[29] A relevant take-away is that current MD systems have significant room for improvement to attain excellent efficiencies, given optimal systems design and further membrane innovations.

For practical systems that can be achieved with real materials, the maximum GOR possible can be modeled, and compared with flux (Fig. 8.11).[13]

As seen in Fig. 8.11, the maximum achievable GOR can be plotted versus flux, and is obtained with optimized membrane thickness. Notably, these efficiencies while achievable, are a significant
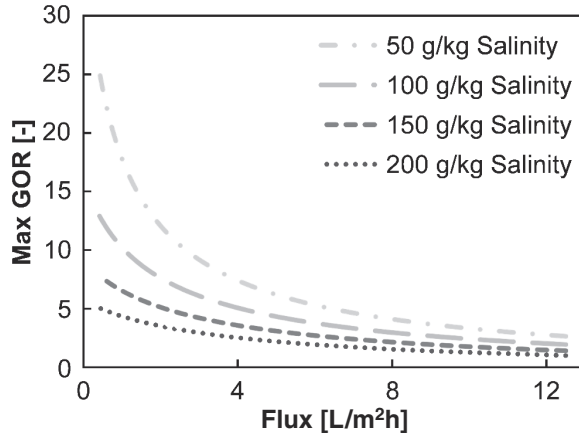
Fig. 8.11. Maximum achievable GOR by using the ideal membrane thickness at each salinity and flux for CGMD.[18]

improvement upon those seen in existing applications, as current products do not optimize membrane thickness for given salinities.

8.2.8. *Performance metric summary*

As a summary, these six parameters provide a comprehensive analysis of MD performance and are all distinctly useful for system design. While flux (J) and overall efficiency (GOR) describe the overall system-level size and energy needs respectively, thermal efficiency η_{th} allows for module-level design especially for the air gap and membrane. On the other hand, and effectiveness (ε) gives insight on the degree of energy recovery and associated temperature differences (ΔT). Through a variety of equations, these parameters can be related to one another, and are detailed in the Section 8.2.6.[10]

8.3. Designing MD Configuration with MD Metrics

The cost of MD is a function of both system capital expenditure (CapEx) and operating expenditure (OpEx), which can be studied from a tradeoff of two metrics for MD performance. First, CapEx is proportional to the system size, and hence inversely related to system productivity, measured by pure water flux. For designing MD systems, the metrics can be summarized and rated for the utility in calculating OpEx, System Side, and Material optimization

Table 8.1. MD metrics and qualitative importance of metrics in design of MD.

Metric	Symbol [unit]	Equation	Average value [lab scale]	Limits	Short definition	Importance in OpEx	Importance in System size	Importance in Material	Refs.
Flux	J [L/m²h]	$J \equiv \dfrac{\dot{m}_p}{A}$ or $J = B_m \Delta P_{vap}$	3-100	NA	Normallized pure water flow rate	★	★★★★	★★★	13,14, 30–36
Gained Output Ratio	GOR [-]	$GOR \equiv \dfrac{\dot{m}_p h_{fg}}{\dot{Q}_H}$	4-13 [<1]	0.1-13 (<860 theoretically)	Energy reuse multiplier	★★★★★	★	★	10,13–18, 23,37–39
Thermal Efficiency	η_{th} [-]	$\eta_{th} = \dfrac{\dot{Q}_{vap}}{\dot{Q}_{vap} + \dot{Q}_{cond}}$	0.6-0.94	<1	Fraction of heat used for desalination	★★★★		★★★★★	113–15,23, 32,35,38
Heat Transfer Effectiveness	ε [-]	$\varepsilon = \dfrac{T_{c,o} - T_{c,i}}{T_{f,i} - T_{c,i}}$	0.7-0.93 [0-0.1]	<1	Fraction of maximum possible heat transfer between feed inlet & outlet	★★★★	★★★★	★	10,12, 13,18,35
Number of Transfer Units	NTU [-]	$NTU = \dfrac{UA}{\dot{m}c_p}$	5-50 [0-0.1]	NA	Dimensionless area and heat transfer parameter	★	★★★★	★★★★★	10,12,13, 18,35
Second Law Efficiency	η_{II} [-]	$\eta_{II} = \dfrac{\dot{Q}_{least}^{min}}{\dot{Q}_H}$	1-12% [0%]	<100%	Universal thermodynamic efficiency	★★★★★	★★★	★★★	17,29, 40–42

(Table 8.1). This summary table gives the units, typical values, limits, and concise definitions for each metric. Also a pictoral representation of each metric is provided, relating them to the key variables and more detailed system diagrams.

The second main metric relates to OpEx, which is mainly representing the cost of energy required to drive the process. In MD, most of the energy supplied is in the form of heat energy, since the pumping power requirement is low in most well-designed MD systems. As a result, OpEx is inversely proportional to the energy efficiency of the system, measured as GOR, thermal efficiency, and second law efficiency.

Acknowledgements

Nomenclature

Symbols

A	Membrane area, m^2
B_m	Membrane permeability, $kg/m^2Pa\,s$
B	Membrane coefficient, $kg/m\,Pa\,s$
BPE	Boiling Point Elevation, °C
c_p	Specific heat capacity at constant pressure, $J/kg\,K$
d	Depth or thickness, m
h	Heat transfer coefficient, W/m^2K
$h_\mathrm{eff,m}$	heat transfer coefficient corresponding to vapor transfer across the membrane, W/m^2K
h_fg	Enthalpy of vaporization, J/kg
g	Specific Gibbs free energy kJ/kg
HX	Heat Exchanger
J	Permeate flux, $kg/m^2\,s$
k	Thermal conductivity, $W/m\,K$
L	Length of module, m

$\dot{m}$	Mass flow rate, kg/s
$\dot{Q}$	Heat transfer rate, W
$\dot{q}$	Heat flux, W/m2
p_{vap}	Vapor Pressure, Pa
S	Entropy J/K
$\dot{S}_{\text{gen}}$	Entropy generation rate W/K
s	Specific entropy J/kg K
SEC	specific energy consumption, kWh/m^3
T	Temperature,°C
T_0	Ambient temperature,°C
U	Overall heat transfer coefficient, W/m^2 K
$\dot{W}$	Work transfer rate [W]
$\dot{W}_{\text{sep}}$	Work of separation [W]
$\dot{W}_{\text{used}}$	Actual work used
w	Module width, m
Greek	
Δ	Change in a variable
ΔP_{vap}	Vapor pressure difference, Pa
δ_{m}	Membrane thickness, m
η_{th}	Thermal efficiency
η_{II}	second law efficiency
ε	Effectiveness

Subscripts

0	Environment, or global dead state
b	Brine
cond	Conduction
eff	Effective
f	Feed
c	Cold
gen	Generated
H	Heat
i	Inlet
m	Membrane
max	Maximum
o	outlet
p	Permeate (product)

S	Solar heat source
sep	Separation
sw	Sea water
th	thermal
v	Vapor
vap	vapor
W	Waste heat source

Acronyms

AGMD	Air gap membrane distillation
CGMD	Conductive gap membrane distillation
DCMD	Direct contact membrane distillation
GOR	Gained output ratio
MD	Membrane distillation
MR	Mass flow ratio
NTU	Number of transfer units
RR	Recovery ratio
PGMD	Permeate gap membrane distillation
VMD	Vacuum membrane distillation

References

1. A. Murena, L. Borea, T. Zarra, J. Boguniewicz-Zablocka, V. Belgiorno, V. Naddeo, Water–Energy Nexus: Evaluation of the Environmental Impact on the National and International Scenarios, in: V. Naddeo, M. Balakrishnan, K.-H. Choo (Eds.), *Frontiers in Water-Energy-Nexus — Nature-Based Solutions, Advanced Technologies and Best Practices for Environmental Sustainability*, Springer International Publishing, 2020, pp. 33–35.

2. R. Damania, The economics of water scarcity and variability, *Oxford Rev. Econ. Policy*, **36** (2020) 24–44. doi:10.1093/oxrep/grz027.

3. A. Alkhudhiri, N. Darwish, N. Hilal, Membrane distillation: A comprehensive review, *Desalination*, **287** (2012) 2–18. doi:10.1016/J.DESAL.2011.08.027.

4. A. Deshmukh, C. Boo, V. Karanikola, S. Lin, A. P. Straub, T. Tong, D. M. Warsinger, M. Elimelech, Membrane distillation at the water-energy nexus: Limits, opportunities, and challenges, *Energy Environ. Sci.*, **11** (2018) 1177–1196. doi:10.1039/c8ee00291f.

5. K. W. Lawson, D. R. Lloyd, Membrane distillation, *J. Memb. Sci.* **124**, 1–25 (1997).

6. D. M. Warsinger, J. Swaminathan, E. Guillen-Burrieza, H. A. Arafat, V. J. H. Lienhard, Scaling and fouling in membrane distillation for desalination applications: A review. Desalination 356, 294–313 (2014).

7. R. Schwantes, A. Cipollina, F. Gross, J. Koschikowski, D. Pfeifle, M. Rolletschek, V. Subiela, Membrane distillation: Solar and waste heat driven demonstration plants for desalination, *Desalination*, **323** (2013) 93–106. doi:10.1016/j.desal.2013.04.011.

8. C. Lienhard, G. P. Thiel, D. M. Warsinger, L. D. Banchik, Low Carbon Desalination: Status and Research, Development, and Demonstration Needs, Report of a workshop conducted at the Massachusetts Institute of Technology in association with the Global Clean Water, *Desalination Alliance*, 2016. http://hdl.handle.net/1721.1/105755.

9. K. S. Pitzer, J. C. Peiper, R. H. Busey, Thermodynamic properties of aqueous sodium chloride solutions, *J. Phys. Chem. Ref. Data.*, **13** (1984) 1–102. doi:10.1063/1.555709.

10. J. Swaminathan, H. W. Chung, D. M. Warsinger, J. H. Lienhard V, Membrane distillation model based on heat exchanger theory and configuration comparison, *Appl. Energy*, **184** (2016) 491–505. doi:10.1016/J.APENERGY.2016.09.090.

11. J. Swaminathan, H. W. Chung, D. M. Warsinger, J. H. Lienhard, Simple method for balancing direct contact membrane distillation, *Desalination*, **383** (2016) 53–59. doi:10.1016/j.desal.2016.01.014.

12. H. Y. Wu, M. Tay, R. W. Field, Novel method for the design and assessment of direct contact membrane distillation modules, *J. Membr. Sci.*, **513** (2016) 260–269. doi:10.1016/J.MEMSCI.2016.04.009.

13. J. Swaminathan, H. W. Chung, D. M. Warsinger, J. H. Lienhard V, Energy efficiency of membrane distillation up to high salinity: Evaluating critical system size and optimal membrane thickness, *Appl. Energy.*, **211** (2018) 715–734. doi:10.1016/J.APENERGY.2017.11.043.

14. J. A. Andrés-Mañas, A. Ruiz-Aguirre, F. G. Acién, G. Zaragoza, Performance increase of membrane distillation pilot scale modules operating in vacuum-enhanced air-gap configuration, *Desalination*, **475** (2020) 114202. doi:10.1016/J.DESAL.2019.114202.

15. D. M. Warsinger, J. Swaminathan, L. L. Morales, J. H. Lienhard V, Comprehensive condensation flow regimes in air gap membrane distillation: Visualization and energy efficiency, *J. Membr. Sci.*, **555** (2018) 517–528. doi:10.1016/J.MEMSCI.2018.03.053.

16. E. K. Summers, H. A. Arafat, J. H. Lienhard, Energy efficiency comparison of single-stage membrane distillation (MD) desalination cycles in different configurations, *Desalination*, **290** (2012) 54–66. doi:10.1016/J.DESAL.2012.01.004.

17. H. W. Chung, J. Swaminathan, D. M. Warsinger, J. H. Lienhard V, Multistage vacuum membrane distillation (MSVMD) systems for high salinity applications, *J. Membr. Sci.*, **497** (2016) 128–141. doi:10.1016/J.MEMSCI.2015.09.009.

18. D. M. Warsinger, G. P. Thiel, J. H. Lienhard V, The Membrane Distillation Efficiency-Flux Frontier, Chevron Rep. CW1251339 (FKA CW793339). (2015).

19. M. Mustakeem, A. Qamar, A. Alpatova, N. Ghaffour, Dead-end membrane distillation with localized interfacial heating for sustainable and energy-efficient desalination. *Water Res.* **189**, 116584 (2021).

20. D. Winter, J. Koschikowski, M. Wieghaus, Desalination using membrane distillation: Experimental studies on full scale spiral wound modules, *J. Membr. Sci.*, **375** (2011) 104–112. doi:10.1016/J.MEMSCI.2011.03.030.

21. J. Swaminathan, H. W. Chung, D. M. Warsinger, V. J. H. Lienhard, Membrane distillation model based on heat exchanger theory and module comparison, *Appl. Energy*, 184, 491–505 (2015).

22. W. Kays, A. London, *Compact Heat Exchangers: A Summary of Basic Heat Transfer and Flow Friction Design Data*, McGraw-Hill, 1958.

23. D. Warsinger, K. Mistry, K. Nayar, H. Chung, J. Lienhard V, Entropy generation of desalination powered by variable temperature waste heat, *Entropy*, **17** (2015) 7530–7566. doi:10.3390/e17117530.

24. J. H. Lienhard IV, J. H. Lienhard V, *A Heat Transfer Textbook*, Dover Publications, Inc, 2011. http://web.mit.edu/lienhard/www/ahtt.html.

25. L. D. Banchik, M. H. Sharqawy, J. H. Lienhard, Effectiveness-mass transfer units (ε-MTU) model of a reverse osmosis membrane mass exchanger, *J. Membr. Sci.*, **458** (2014) 189–198. doi:10.1016/J.MEMSCI.2014.01.039.

26. M. H. Sharqawy, L. D. Banchik, J. H. Lienhard, Effectiveness–mass transfer units (ε–MTU) model of an ideal pressure retarded osmosis membrane mass exchanger, *J. Membr. Sci.*, **445** (2013) 211–219. doi:10.1016/J.MEMSCI.2013.06.027.

27. S. Al-Obaidani, E. Curcio, F. Macedonio, G. Di Profio, H. Al-Hinai, E. Drioli, Potential of membrane distillation in seawater desalination: Thermal efficiency, sensitivity study and cost estimation, *J. Membr. Sci.*, **323** (2008) 85–98. doi:10.1016/J.MEMSCI.2008.06.006.

28. S. Lin, N. Y. Yip, M. Elimelech, Direct contact membrane distillation with heat recovery: Thermodynamic insights from module scale modeling, *J. Membr. Sci.*, **453** (2014) 498–515. doi:10.1016/J.MEMSCI.2013.11.016.

29. K. H. Mistry, R. K. McGovern, G. P. Thiel, E. K. Summers, S. M. Zubair, J. H. Lienhard V, Entropy generation analysis of desalination technologies, *Entropy*, **13** (2011) 1829–1864. doi:10.3390/e13101829.

30. A. E. Khalifa, Flux enhanced water gap membrane distillation process-circulation of gap water, *Sep. Purif. Technol.*, **231** (2020). doi:10.1016/j.seppur.2019.115938.

31. S. M. Alawad, A. E. Khalifa, Analysis of water gap membrane distillation process for water desalination, *Desalination*, **470** (2019). doi:10.1016/j.desal.2019.114088.

32. R. Schwantes, L. Bauer, K. Chavan, D. Dücker, C. Felsmann, J. Pfafferott, Air gap membrane distillation for hypersaline brine concentration: Operational analysis of a full-scale module–New strategies for wetting mitigation, *Desalination*, **444** (2018) 13–25. doi:10.1016/j.desal.2018.06.012.

33. R. Miladi, N. Frikha, A. Kheiri, S. Gabsi, Energetic performance analysis of seawater desalination with a solar membrane distillation, *Energy Convers. Manag.*, **185** (2019) 143–154. doi:10.1016/j.enconman.2019.02.011.

34. L. Gao, J. Zhang, S. Gray, J. De Li, Influence of PGMD module design on the water productivity and energy efficiency in desalination, *Desalination*, **452** (2019) 29–39. doi:10.1016/j.desal.2018.10.005.

35. J. Swaminathan, J. H. Lienhard, Design and operation of membrane distillation with feed recirculation for high recovery brine concentration, *Desalination*, **445** (2018) 51–62. doi:10.1016/j.desal.2018.07.018.

36. D. Winter, J. Koschikowski, M. Wieghaus, Desalination using membrane distillation: Experimental studies on full scale spiral wound modules, *J. Memb. Sci.*, **375** (2011) 104–112.

37. H. B. Parmar *et al.*, Nanofluids improve energy efficiency of membrane distillation, *Nano Energy* (2021).

38. J. Swaminathan, J. H. Lienhard, Energy efficiency of sweeping gas membrane distillation desalination cycle. in (Proceedings of the 22nd National and 11th International ISHMT-ASME Heat and Mass Transfer Conferencer, 2013).

39. J. Swaminathan *et al.* Energy efficiency of permeate gap and novel conductive gap membrane distillation, *J. Memb. Sci.*, **502** (2016) 171–178.

40. A. Deshmukh, M. Elimelech, Understanding the impact of membrane properties and transport phenomena on the energetic performance of membrane distillation desalination, *J. Memb. Sci.*, **539** (2017) 458–474.

41. K. H. Mistry, J. H. Lienhard, Generalized least energy of separation for desalination and other chemical separation processes, *Entropy*, **15** (2013) 2046–2080.

42. G. P. Thiel, E. W. Tow, L. D. Banchik, H. W. Chung, J. H. Lienhard, Energy consumption in desalinating produced water from shale oil and gas extraction, *Desalination*, **366** (2015) 94–112.